The American Journal of Pathology, Vol. 182, No. 6, June 2013

The American Journal of
PATHOLOGY
ajp.amjpathol.org

BIOPHYSICAL IMAGING AND COMPUTATIONAL BIOLOGY

Anti—IL-17A Treatment Reduces Clinical Score and VCAM-1 Expression Detected by *in Vivo* Magnetic Resonance Imaging in Chronic Relapsing EAE ABH Mice

Silvy Mardiguian,* Sébastien Serres,† Emma Ladds,‡ Sandra J. Campbell,* Panop Wilainam,* Charles McFadyen,* Martina McAteer,§ Robin P. Choudhury,§ Paul Smith,¶ Fay Saunders,‖ Gillian Watt,** Nicola R. Sibson,† and Daniel C. Anthony*

From the CR-UK/MRC Gray Institute for Radiation Oncology and Biology, the Departments of Pharmacology† and Cardiovascular Medicine,§ and the Clinical Medical School,‡ Magdalen College, University of Oxford, Oxford; the Department of Pharmacology,¶ UCB Pharma S.A., Great Abingdon; and the Departments of Antibody Biology‖ and Pharmacology,** UCB Pharma S.A., Slough, United Kingdom*

Accepted for publication February 21, 2013.

Address correspondence to Daniel Anthony, Ph.D., Department of Pharmacology, University of Oxford, Oxford OX1 3QT, UK. E-mail: daniel.anthony@pharm.ox.ac.uk.

IL-17 is argued to play an important role in the multiple sclerosis—like disease experimental autoimmune encephalitis (EAE). We investigated the therapeutic effects of anti—IL-17A in a chronic relapsing EAE ABH mouse model using conventional scoring, quantitative behavioral outcomes, and a novel vascular cell adhesion molecule 1 (VCAM-1)—targeted magnetic resonance imaging (MRI) contrast agent [anti—VCAM—microparticles of iron oxide (MPIO)] to identify conventionally undetectable neuropathology. Mice were administered prophylactic or treatment regimens of anti—IL-17A or IgG and two injections of anti—VCAM-MPIO before undergoing T2*-weighted three-dimensional and gadolinium—diethylenetriamine pentaacetic acid T1-weighted MRI. Rotarod, inverted screen, and open field motor function tests were performed, conventional clinical scores calculated, and central IL-17A mRNA expression quantified during acute disease, remission, and relapse. Prophylactic anti—IL-17A prevents acute disease and relapse and is associated with reduced clinical and functional severity. Treatment regimens delay relapse, improve functional scores, and are associated with reduced VCAM-MPIO lesions during remission. No significant alteration was detectable in levels of gadolinium—diethylenetriamine pentaacetic acid— or VCAM-MPIO—positive lesions during relapse. Prophylactic and treatment anti—IL-17A were therapeutically effective in chronic relapsing EAE, improving clinical and quantifiable functional outcomes. IL-17A expression seems significant during acute disease but less important chronically. Disease-related immunoneuropathology is more sensitively detected using VCAM-MPIO MRI, which may, therefore, be used to monitor therapy meaningfully. *(Am J Pathol 2013, 182: 2071—2081; http://dx.doi.org/10.1016/j.ajpath.2013.02.029)*

Multiple sclerosis (MS) and the MS-like disease experimental autoimmmune encephalitis (EAE) are chronic inflammatory disorders of the central nervous system (CNS) associated with demyelination and axonal injury,[1] neurologic disability, and subsequent sensory and motor functional disability, which may adopt relapsing-remitting or progressive patterns. Despite extensive investigation, the exact immunopathogenic mechanisms, particularly the role of IL-17A compared with other IL-17 family members underlying the conditions, remain imperfectly understood.

Conventionally, an important role is ascribed to $CD4^+$ interferon-γ—producing myelin-reactive T_H1 cells,[2] with the polarizing factor IL-12 enhancing encephalitogenicity.[3] However, IL-12 knockout mice, incapable of producing T_H1 cells, are still susceptible to EAE,[4] suggesting that these cells are not solely responsible and prompting the search for additional contributors. Several studies have now shown that IL-23—polarized T_H17 cells, which produce IL-17, can play an important role in EAE. T_H17 depletion from the T-cell repertoire abolishes the induction of EAE in naive syngeneic hosts after adoptive transfer, whereas IL-23—modulated T_H17 cells are capable of transferring the condition.[5] The IL-17—producing $CD8^+$ T (Tc17) cells have also been shown to be

Supported by Medical Research Council research grant G0401438 and The Wellcome Trust (R.P.C.).

http://dx.doi.org/10.1016/j.ajpath.2013.02.029

required for EAE induction and for promotion of T_H17 accumulation in the CNS.[6] Furthermore, IL-17 has been shown to alter characteristics of EAE, with administration of an IL-17 receptor—Fc protein or antibody reducing disease severity[7,8] and an anti—IL-23 antibody preventing EAE relapse, likely by the suppression of IL-17.[9] However, the effects of anti—IL-17 in these studies were quite modest, and, hitherto, the effect of suppressing IL-17A in relapsing disease is unknown.

The complexity of the interweaving web of cytokines contributing to disease pathogenesis is becoming apparent, as is the increasing likelihood of temporal specificity for the dominant effects of individual contributors. For example, IL-23—deficient mice are completely resistant to EAE,[10] whereas IL-17A/F knockout mice have been shown to be susceptible.[11,12] Possible explanations for this discrepancy could include compensatory up-regulation of alternative signaling pathways after genetic manipulation or parallel co-contributing IL-17—dependent and IL-17—independent pathways.[13]

Antagonist studies, which result in fewer confounding effects and, therefore, produce arguably more compelling data, have shown that IL-17 inhibition with neutralizing antibodies is effective at suppressing EAE,[9,14] although only partially in mice that have received IL-23—modulated effector T cells.[3] Moreover, one study reported that anti—IL-17 therapy resulted in therapeutic benefits in experimental autoimmune uveitis, whereas IL-17 genetic deficiency did not abrogate experimental autoimmune uveitis susceptibility.[15] Mechanistically, IL-17A production in CNS-infiltrating T cells has been associated with blood-brain barrier (BBB) disruption and disease activity[16] and the suppression of Act1 signaling, downstream of the IL-17RA, in astrocytes reduces the number of infiltrating cells.[17] Therefore, IL-17 remains an interesting therapeutic target in these chronic inflammatory conditions.

We recently demonstrated that using a novel vascular cell adhesion molecule 1 (VCAM-1)—targeted magnetic resonance imaging (MRI) contrast agent [VCAM—microparticles of iron oxide (MPIO)], it is possible to detect endothelial activation and VCAM-1 expression *in vivo*.[18] This approach has multiple advantages compared with conventional imaging techniques, such as passive contrast gadolinium—diethylenetriamine pentaacetic acid (Gd-DTPA) enhancement. Not only does the use of a targeted agent reveal gray and white matter lesions irrespective of their size or position in the CNS, but, more important, it also enables the volumetric detection of EAE lesions at a time when conventional, clinically used MRI techniques do not reveal abnormalities.[19] In particular, we have shown that inflammatory foci containing cuffs of leukocytes around vessels are VCAM-MPIO positive but Gd-DTPA negative.[19] This finding facilitates serial quantitation of EAE lesion load throughout disease progression and the objective evaluation of potential therapeutic agents on the pathologic process during subclinical stages,[20] a facility that is going to become of increasing relevance and usefulness in the future.

The aims of this study were fourfold: i) to confirm and compare the effectiveness of prophylactic and therapeutic regimens of anti—IL-17A therapy in a chronic relapsing (CR)-EAE model; ii) to identify a sensitive quantifiable measure of motor function and examine the correlation with conventional clinical scores during the disease course; iii) to compare the correlation between demonstrable MRI lesion load using VCAM-MPIO and Gd-DTPA imaging techniques and the association with conventional scoring and motor outcome measures; and iv) to quantify the levels of IL-17A present during different disease stages to assess its potential pathologic contribution.

Materials and Methods

Animals

All the animals were fed standard food and water *ad libitum*. Animal care and procedures were performed according to the UK Home Office protocols and guidelines. Six- to ten-week-old female adult Biozzi antibody high (ABH) mice (Charles River Laboratories, Kent, UK) were allocated to four groups by random number selection: control ($n = 12$) + control EAE ($n = 10$), prophylactic regimen ($n = 23$), and treatment regimen ($n = 70$). All the antibodies (UCB, Slough, UK) were administered s.c. at a dose of 30 mg/kg.

Pharmacologic Protocols

Group 1 control animals ($n = 8$) received complete Freund's adjuvant (CFA) (Sigma-Aldrich, Dorset, UK) on post-sensitization days (PSDs) 0 and 7, and these animals received no other treatment. For group 2, CR-EAE was induced (see the next subsection) ($n = 10$), but no Ig was administered. This group controlled for the repeated stress of the Ig injections on CR-EAE pathogenesis. CR-EAE was induced in groups 3 ($n = 10$) and 4 ($n = 10$), and these animals received eight doses of either IgG or anti—IL-17A on PSDs 1, 6, 12, 20, 26, 33, 40, and 47. Group 5 consisted of untreated naive animals ($n = 3$). Under the treatment administration regimens, groups 6 ($n = 4$) and 7 ($n = 5$) received four doses of either IgG or anti—IL-17A on PSDs 28, 35, 42, and 49 only (ie, commencing in the period of remission). For groups 8 ($n = 24$) and 9 ($n = 25$), CR-EAE was induced and IgG or anti—IL-17A was administered as for groups 6 and 7. A rescue administration protocol was used for groups 10 ($n = 6$) and 11 ($n = 6$), in which CR-EAE had been induced on PSDs 0 and 7, and IgG or anti—IL-17A was administered on PSDs 17, 24, 31, and 38 (ie, from peak disease onward).

CR-EAE

CR-EAE was induced by s.c. injection into both abdominal flanks of 0.15 mL of an emulsion consisting of 500 μg of mouse spinal cord homogenate in CFA supplemented with

mycobacteria (*Mycobacterium tuberculosis* and *Mycobacterium butyricum*) (Difco Laboratories, Detroit, MI).

Animals were injected on PSDs 0 and 7 and were weighed and assessed daily for clinical signs according to the following guidelines: grade 0 indicates healthy; grade 1, flaccid tail; grade 2, incomplete hindlimb paralysis; grade 3, complete hindlimb paralysis; and grade 4, forelimb paralysis/moribund. Any animal judged to be grade 4 severity was culled immediately.

Quantitative Motor Functional Tests

All the tests were performed as in the study by Guenther et al,[21] with minor modifications.

Rotarod Test

Mice were placed on a grooved tube rotating at 4 rpm that accelerated at 20 rpm/min to a maximum speed of 40 rpm and were removed after 120 seconds. The time until a mouse first slipped, time spent on the rotarod, number of slips (double hindlimb footfalls), and time a mouse spent gripping the rod and going in circles were recorded. Animals were also tested on static rods, but the results were the least discriminatory of motor function and the data are not shown.

Inverted Screen Test

Mice were placed on a square of wire mesh screen (50 × 50 cm) surrounded by a 4-cm-wide wooden edge to prevent animals from climbing over to the other side. The screen was turned upside down above soft padding. After 120 seconds it was rotated back, and the mouse was removed. The time taken for the hindlimbs to drop from the screen, the time before a mouse fell, and the distance traveled on the inverted screen were recorded.

Open Field Test

Mice were placed into a rectangular wooden box (50 × 70 cm) with 3-cm-deep soiled bedding (from cages of female littermates) and were allowed to explore for 180 seconds. A given mouse never encountered the same bedding twice to avoid habituation.[22] The number of squares crossed, rears, burrows, and distance traveled were recorded. Open field tests were performed on PSDs 1, 4, 7, 10, 12, 14, 20, 27, 34, 38, 41, 45, and 48.

Antibody Conjugation to MPIO and Imaging

Purified monoclonal rat antibodies specific to mouse VCAM-1 (clone M/K2; Cambridge Bioscience, Cambridge, UK) or control IgG-1 (clone Lo-DNP-1; AbD Serotec, Raleigh, NC) were conjugated to MyOne tosylactivated MPIO (1-μm diameter; iron content, 26%) with p-toluenesulphonyl (tosyl)-reactive surface groups (Invitrogen, Carlsbad, CA) as described previously.[16]

On PSDs 28 and 42, ABH mice were anesthetized with 1% to 2% isoflurane in 100% O_2, were injected intravenously with 100 μL of sterile saline containing 4 mg of Fe/1 kg of anti−VCAM-1−MPIO (VCAM-MPIO), and underwent MRI 1 hour later. Mice were positioned in a 2.6-cm i.d. quadrature birdcage coil (Rapid26; RAPID MR International, Columbus, OH). Electrocardiography was monitored throughout, and body temperature was maintained at approximately 37°C. MRI data were acquired using a 7-T horizontal bore magnet with a Varian Inova spectrometer (Varian Inc., Palo Alto, CA).

Magnetic Resonance Imaging

Scout images were acquired to position the center of the brain in the middle of the magnet. Subsequently, a T2*-weighted three-dimensional gradient echo data set was acquired with the following parameters: flip angle, 31°; repetition time, 50 milliseconds; echo time, 5 milliseconds; field of view, 11.2 × 22.5 × 22.5 mm; matrix size, 96 × 192 × 256; two averages; and total acquisition time, approximately 40 minutes. The means ± SEM midpoint of acquisition was 1.5 ± 0.1 hours after MPIO injection.

The data were zero filled to 128 × 256 × 256 and were reconstructed offline, giving a final isotropic resolution of 88 μm. A single 1-mm horizontal section was acquired using a fast spin-echo T2-weighted sequence (repetition time = 3.0 milliseconds; echo time = 40 milliseconds) to enable the positioning of 11 × 1-mm coronal sections for T1-weighted imaging. Spin-echo T1-weighted images (repetition time = 500 milliseconds; echo time = 13 milliseconds) were acquired before and 5 minutes after a bolus i.v. injection of 30 μL (1.2 mL/kg) of Gd-DTPA (Omniscan; GE Healthcare, Chalfont St. Giles, UK) to identify BBB permeability, equivalent to twice the high dose that is used in humans for MS lesion detection.[23]

MRI Data Analysis

T2*-Weighted Anti−VCAM-MPIO Images

T2*-weighted three-dimensional images were processed into a three-dimensional isotropic data set and converted into TIFF image files. For each image, the brain was manually masked to exclude extracerebral structures. Individual sections were then converted to 8-bit grayscale and thresholded in the gray channel at the same level using Adobe Photoshop software version CS2 (Adobe Systems Europe Ltd., Maidenhead, UK).

Quantification of anti−VCAM-MPIO binding (defined as focal hypointensities) was performed by observers masked to the identity of the data set. Anti−VCAM-MPIO binding was quantified in 256 consecutive brain sections for each animal. Segmented images were reconstructed using the 3D Constructor plug-in for Image-Pro Plus (Media Cybernetics Inc., Rockville, MD) to visualize the distribution of MPIO binding throughout the brain, with low-signal areas assigned to the red channel and the anatomical images to the green channel. Voxel volumes were then summed and expressed

as raw volumes in microliters, with no surface rendering or smoothing effects. The three-dimensional reconstructions of VCAM-MPIO binding were then subtracted from the signal arising from sinuses, which likely resulted from blood pooling.

T1-Weighted Gd-DTPA Contrast-Enhanced Images

Gd-DTPA contrast enhancement on T1-weighted images was defined as regions of hyperintensity and was quantified in 11 consecutive brain sections for each animal. These volumes were then subtracted from the average volume of Gd enhancement in three naive ABH mice injected with Gd.

RNA Extraction and Real-Time PCR

RNA extraction and real-time quantitative PCR assays were performed from pieces of snap-frozen brain as previously described,[24] with standard curves generated from reverse-transcribed single-stranded RNA produced from T7 templates for each probe set.[25] Results are expressed as number of copies of target per nanogram of input RNA corrected to the housekeeping gene glyceraldehyde-3-phosphate dehydrogenase.

Statistical Analysis

Statistical analysis was performed using SPSS software version 19 (SPSS Inc., Chicago, IL). Paired-samples *t*-tests or *U*-tests were used to identify differences between the groups for parametric or nonparametric parameters, respectively. Data are expressed as means ± SEM, and statistical significance was assigned at $P < 0.05$. Results were analyzed in an intention-to-treat manner, with dead animals included in the respective cohort figures.

Results

Prophylactic Administration of Anti–IL-17A in a CR-EAE Model Prevents Development of Acute Disease and Subsequent Relapse and Improves Clinical Outcomes

This study aimed to evaluate the therapeutic effects of prophylactic anti–IL-17A treatment on disease course and progression in a CR-EAE model. Assessment of treatment was made by calculating mean clinical cohort scores and disability ratings over particular stages of the EAE illness: the acute phase, PSDs 13 to 30 (PSDs 13 to 25 in the prophylactic regimen); remission, PSDs 31 to 40; and second relapse, PSDs 41 to 50.

Acute disease developed in all the EAE control animals by PSD 17 and in all those treated with the IgG antibody regimen by PSD 16 (Figure 1A). In contrast, 40% of mice that received prophylactic anti–IL-17A did not show signs of acute disease and remained well, with an undetectable clinical score. EAE mice administered anti–IL-17A that did display signs of acute disease had a significantly lower means ± SEM score than those that received IgG: 0.98 ± 0.11 compared with 0.57 ± 0.17 ($P = 0.043$). Similarly, anti–IL-17A–treated mice exhibited significantly reduced disability on 7 individual days during the acute illness phase (PSDs 15 to 18 and 20 to 22; $P < 0.5$), which was confirmed with Kaplan-Meier plots for animals scoring >1 on a Mantel-Cox test ($P = 0.0082$).

Anti–IL-17A was effective in preventing relapse completely (PSDs 30 to 50) in all but one of the EAE mice that had become disabled during the acute phase, whereas 60% of the IgG-treated animals and EAE controls showed signs of a spontaneous relapse. Moreover, clinical scores were significantly lower ($P < 0.05$) in anti–IL17A–treated mice compared with those given IgG on PSDs 48 to 50, ie, during disease relapse (Figure 1A).

Weight loss is often recorded during the analysis of EAE disease progression because it acts as a quantitative surrogate marker for disease severity. Mice treated prophylactically with anti–IL-17A lost up to 5% of their baseline weight during the acute disease phase compared with EAE controls and those treated with IgG, with the average loss in

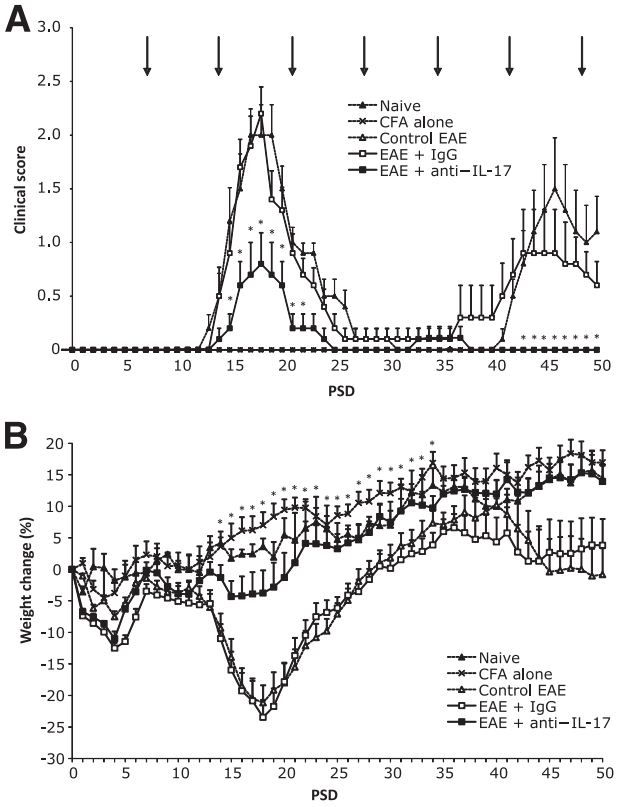

Figure 1 Prophylactic therapy with anti–IL-17A reduces clinical disability and reverses weight loss. **A:** Clinical scores in each group from PSDs 0 to 50. Scores in EAE animals treated with anti–IL-17A were significantly lower than those in mice treated with an IgG control. $n = 10$ in the control EAE, EAE+anti–IL-17A, and EAE+IgG groups; $n = 3$ in the naive group. **Arrows** indicate the day of antibody administration (PSD 1 dose not shown). **B:** Weight change in the groups from PSD 0 to 50. Compared with EAE+IgG-treated mice, EAE+anti–IL-17A–treated mice lost less weight during the acute phase, began to gain weight earlier, did not show prerelapse weight loss, and had significantly greater weight gain on PSDs 14 to 34. Data are shown as means ± SEM. *$P < 0.05$.

both groups being almost 25% (Figure 1B). Furthermore, anti−IL-17A−treated mice gained significantly more weight over PSDs 14 to 34, began to gain weight earlier than the other groups (ie, from PSD 17 compared with PSD 20), and did not experience the prerelapse weight loss seen in EAE controls and IgG-treated animals from PSD 36.

Prophylactic Administration of Anti−IL-17A in a CR-EAE Model Improves Functional Motor Outcomes

Three different motor tests were used in this study to acquire a more objective and quantitative assessment of disease severity: the inverted screen, which tests coordinated movement and strength; the rotarod, which tests balance, coordination, and motor planning; and the open field test as a measure of general activity and behaviors such as rearing and burrowing. Different outcome measures were recorded for each to identify the most sensitive measure of motor function, eg, total time on rotarod and time to first footfall.

In all the recorded outcome measures, the performance of CFA control animals did not deviate from that at baseline. In contrast, the inverted screen and rotarod tests revealed a significant quantitative difference in performance between the anti−IL-17A and IgG treatment groups during the acute disease and relapse phases (Figure 2). Anti−IL-17A animals spent longer on the inverted screen and rotarod and continued on for longer before the first footfall.

Time until first footfall on the rotarod was the most sensitive measure for discriminating between the treatment groups, whereas those in the open field test proved least sensitive. However, note that significantly more rears were observed on preclinical PSD 14 onward in the anti−IL-17A−treated group compared with the other EAE treatment groups (Supplemental Figure S1).

Anti−IL-17A Administration after the Acute Disease Phase Prolongs Remission and Reduces Relapse Functional Disability

EAE disease severity has previously been shown to be reduced by anti−IL-17A therapy in a monophasic EAE model.[7] Herein, we were interested to discover whether we could suppress relapse in CR-EAE. After administration of antibodies from PSD 28, ie, during remission of established CR-EAE disease, IgG-treated mice relapsed 2 days earlier than those given anti−IL-17A (means ± SEM PSD 37.4 ± 6.09 versus 39.8 ± 7.20) and exhibited a higher level of disability during relapse, with a maximum mean clinical score on PSD 39 almost twice that of the anti−IL-17A−treated mice (Figure 3A). The first IgG-treated mouse relapsed on PSD 32, and from this point clinical scores were higher in that group on all days, becoming statistically significance on PSDs 37 to 41 and 43. In addition, anti−IL-17A−treated mice gained more weight than IgG mice, although this difference was not statistically significant (Figure 3B).

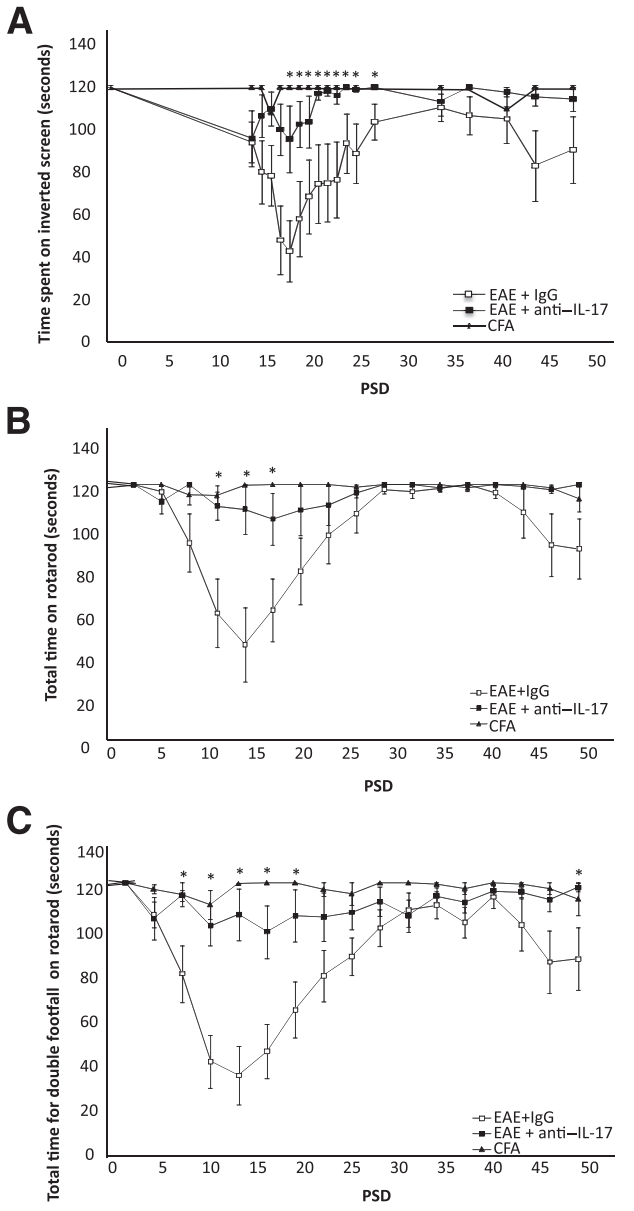

Figure 2 Anti−IL-17A prophylaxis improves motor task performance. **A**: Time spent on the inverted screen. Note that the EAE+anti−IL-17A group remained on the inverted screen for longer than IgG-treated animals during the acute phase of disease. **B** and **C**: EAE+anti−IL-17A−treated animals also displayed a significant improvement on the rotarod, where total time spent (**B**) and time for the first footfall (**C**) in EAE+anti−IL-17A mice were significantly better in the acute phase. Data are shown as means ± SEM. $n = 10$ in the control EAE, EAE+anti−IL-17A, and EAE+IgG groups; $n = 8$ in the CFA control group. $^*P < 0.05$.

Motor testing was performed three times before treatment (PSDs 13, 16, and 20) and three times after treatment (PSDs 34, 37, and 41) (Figure 4). CFA controls scored consistently well on all three motor tests; however, the inverted screen and rotarod tests revealed differences in motor performance consistent with the observed differences in clinical scores. Anti−IL-17A−treated mice spent longer on the screen overall than IgG-treated mice and had a longer interval before their hind legs fell, statistically significant on PSDs

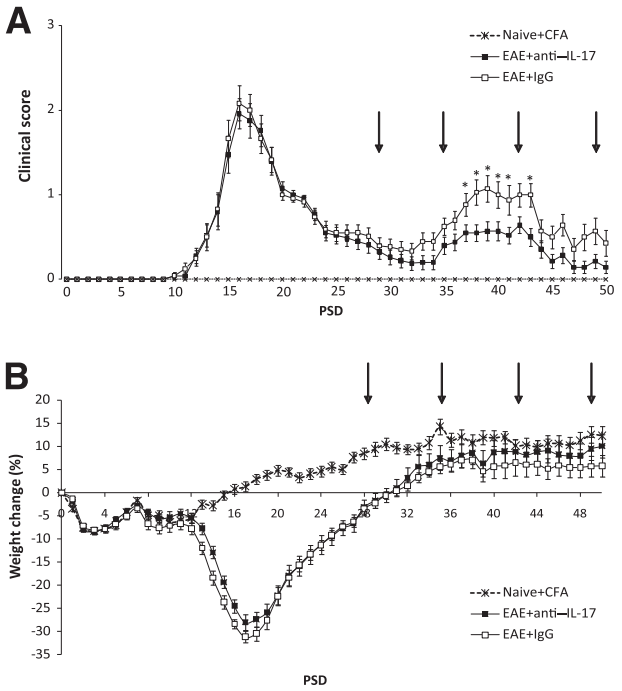

Figure 3 Administration of anti–IL-17 treatment inhibits relapse. **A:** Clinical scores for animals treated from PSD 28. IL-17A–treated animals were less disabled and relapsed later than those that received control IgG. $*P < 0.05$ EAE+anti–IL-17A versus EAE+IgG control mice. **B:** Record of the weights of the animals revealed no significant differences between animals with EAE. Data are shown as means ± SEM. $n = 25$ in the EAE+anti–IL-17A group; $n = 24$ in the EAE+IgG group; $n = 12$ in the CFA control and naive group. **Arrows** indicate the day of administration of vehicle or anti-1L-17A.

37 and 41 (Figure 4A). Similarly, anti–IL-17A–treated mice performed statistically significantly better than their IgG counterparts on the rotarod on the same days (Figure 4B), suggesting that they not only had greater strength but also better levels of coordination and limb control during the clinically defined relapse phase.

Unlike the results on the motor tests, the traditional EAE clinical scoring scheme did not reveal any differences between the treatment groups on PSD 37 as the animals were still asymptomatic. This finding suggests that the motor tests can produce a quantitative outcome measure that is more sensitive than traditional EAE disease scoring, with time to first footfall on the rotarod test being particularly revealing.

Anti–IL-17A Administration during Acute Disease Reduces Clinical Severity during Subsequent Remission and Relapse

The previous elements of the study have shown that anti–IL-17A suppresses the acute and relapse phases of disease if the therapy is initiated in the period with no clinical signs. Herein, we sought to confirm the therapeutic efficacy of a treatment regimen in a CR-EAE model where animals were treated from peak disease. Antibody was administered every 7 days from PSD 17. In this rescue treatment regimen, the acute disease phase was comparable for both groups of EAE mice, with weight losses beginning on PSD 7, disability appearing 2 days later, and peak clinical scores on PSD 16 (Figures 5A). CFA controls all had clinical scores of zero throughout but did initially lose some weight, which was later regained (Figure 5B).

After the peak of the acute disease phase at PSD 16, both groups entered remission. Anti–IL-17A–treated animals returned to baseline more rapidly and exhibited lower means ± SEM clinical scores throughout remission than their IgG-treated counterparts (0.7 ± 0.2 versus 0.2 ± 0.1; $P < 0.05$). On PSD 33, both groups started to relapse. However, although in the IgG-treated group this relapse was sustained until the end of the experimental period, the anti–IL-17A–treated group experienced a transient relapse with complete recovery by PSD 38 (Figure 5A). As illustrated in Figure 5A, after each administration of anti–IL-17A, the clinical score was significantly reduced compared with IgG-treated controls, particularly apparent during the relapse phase.

A marked decrease (maximum 25% to 30%) in body weight was observed in both groups from PSDs 13 to 17, ie, during the acute disease phase in the absence of treatment. However, weight returned to control levels by PSD 28 and

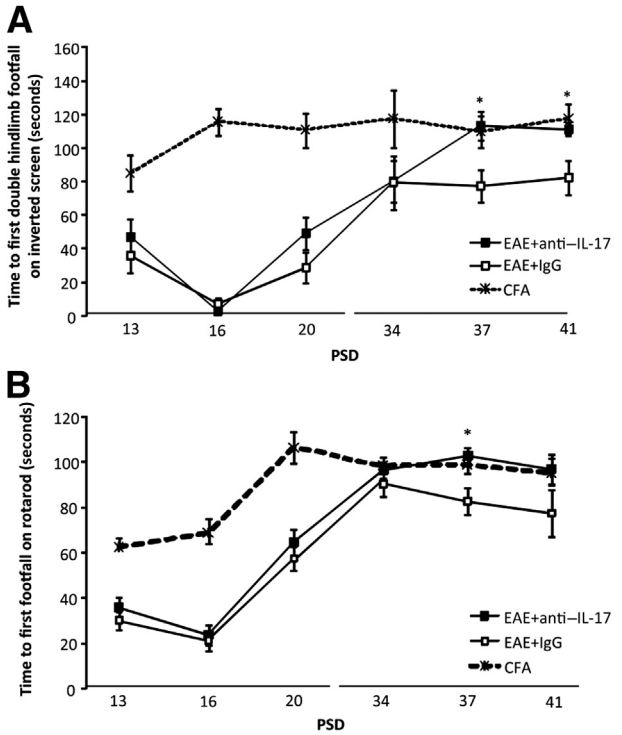

Figure 4 Anti–IL-17A treatment after acute disease improves motor task performance. **A:** Inverted screen performance. The EAE+anti–IL-17A group remained on the inverted screen for longer before a double hindlimb footfall and remained on the screen for longer than IgG-treated animals on PSDs 37 and 41. **B:** Rotarod performance. EAE+anti–IL-17A–treated animals also displayed an improvement on PSDs 37 and 41. Note that both groups were comparable during the acute phase of disease (PSDs 13, 16, and 20) compared with CFA controls. Data are shown as means ± SEM. $n = 25$ in the EAE+anti–IL-17A group, $n = 24$ in the EAE+IgG group; $n = 12$ in the CFA group. $*P < 0.05$ EAE+anti–IL-17A versus EAE+IgG.

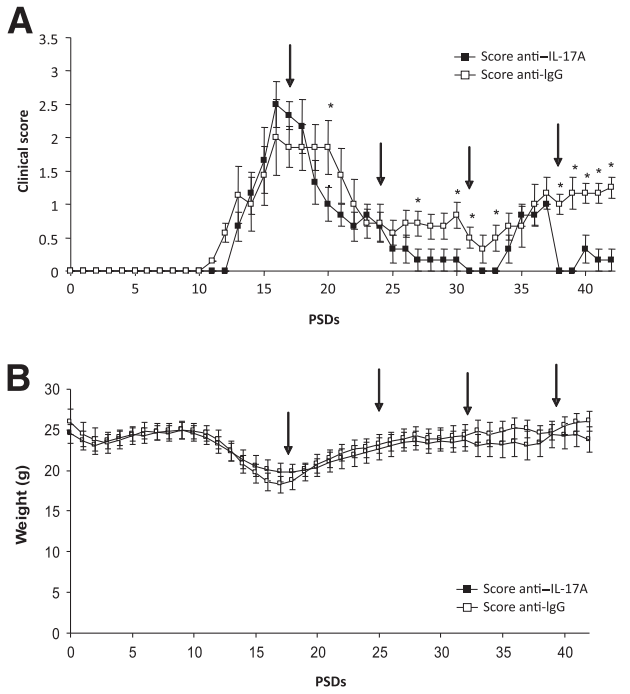

Figure 5 Treatment at peak disease. **A:** Clinical scores of CR-EAE ABH animals treated with IgG (control) or anti−IL-17A ($n = 6$ in each group). Administration of anti−IL-17A on PSDs 17, 24, 31, and 38 (**arrows**) resulted in improved clinical scores, with quicker remission and minimal relapse. *$P < 0.05$. **B:** Body weight in CR-EAE ABH mice treated with IgG (control) or anti−IL-17A. During the acute phase of EAE, a marked reduction in body weight was evident in all the animals, which subsequently returned to control levels throughout remission and subsequent relapse. No significant differences in weight were observed between the treatment groups. Data are shown as means ± SEM.

remained constant during remission and subsequent relapse, with no significant differences found between anti−IL-17A− and IgG-treated animals (Figure 4B).

Anti−IL-17A Treatment Decreases VCAM-MPIO Binding and Gd-DTPA−Enhancing Lesions in CR-EAE ABH Mice during Remission but Not Relapse

The rescue administration protocol was used in the MRI studies. IgG or anti−IL-17A was administered on PSDs 17, 24, 31, and 38 (ie, from peak disease onward), and animals were imaged on PSDs 28 and 42. As previously demonstrated,[19] binding of VCAM-MPIO to the vascular endothelium *in vivo* was evident as focal hypointensities on T2*-weighted images owing to the paramagnetic effects of the iron oxide microparticles (Figure 6, A−H). On PSD 28, the presence of VCAM-MPIO binding in the cortex/striatum, hippocampus/thalamus, midbrain, and cerebellum/medulla (Figure 6, A−D, respectively) of anti−IL-17A−treated mice was more pronounced, as assessed by blinded observers (D.A. and N.R.S.), than in IgG-treated mice at the same levels (Figure 6, E−H). Furthermore, the spatial distribution and extent of VCAM-MPIO binding, visualized by three-dimensional reconstruction (Figure 6, I−L), were significantly lower in anti−IL-17A−treated mice ($P = 0.013$) during remission on PSD 28 than in IgG-treated controls. VCAM-MPIO binding remained significantly elevated over baseline on PSD 42. On PSD 42, no significant differences in VCAM-MPIO binding were observed between anti−IL-17A−treated and control mice (Figure 6M).

Post−Gd-DTPA T1-weighted images were also acquired on PSDs 28 and 42 to examine the extent of BBB breakdown and to compare regional enhancement with VCAM-MPIO binding. Post−Gd-DTPA T1-weighted images showed a significant increase in the number of enhancing lesions (ie, BBB breakdown) in IgG-treated mice on PSD 28 compared with anti−IL17A−treated mice, which showed no breakdown. However,

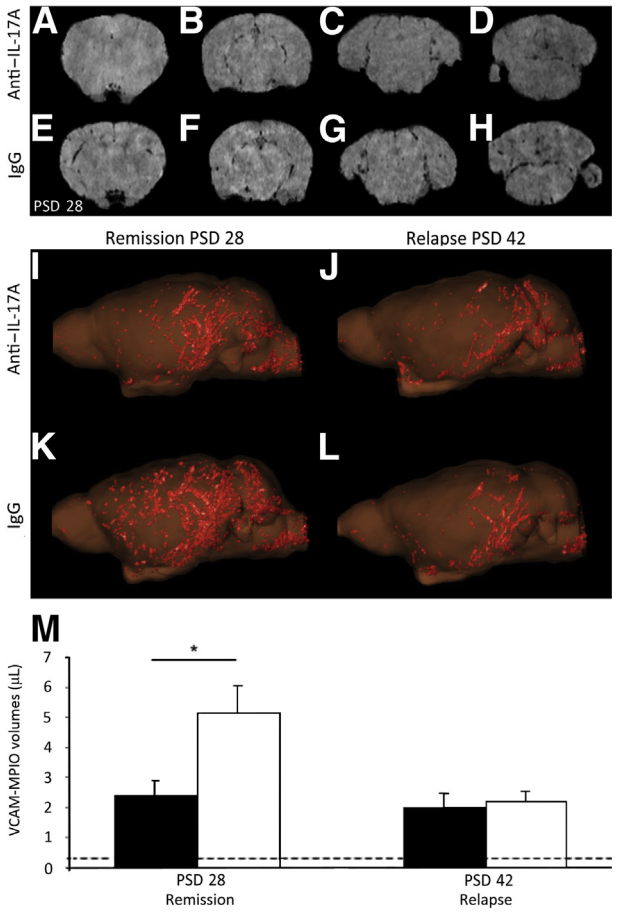

Figure 6 Anti−IL-17A treatment decreased VCAM-MPIO binding in CR-EAE mice on PSD 28. **A**−**H:** Images showing the interaction of VCAM-MPIO with VCAM-1 expressed on the endothelial surface detected as focal hypointensities on T2*-weighted images. On PSD 28, in mice treated with anti−IL-17A, the presence of MPIO binding in the cortex/striatum (**A**), hippocampus/thalamus (**B**), midbrain (**C**), and cerebellum/medulla (**D**) was reduced compared with mice treated with IgG at the same level (**E**−**H**). **I**−**L:** Three-dimensional reconstruction showing that anti−IL17A−treated mice (**I**) exhibited less MPIO binding during remission (PSD 28) than IgG-treated mice (**K**). On PSD 42, no significant differences in MPIO binding were observed (**J** and **L**, respectively). **M:** A significant reduction in VCAM-MPIO binding in anti−IL-17A−treated animals (black bars) was found compared with IgG-treated controls (white bars) on PSD 28, but no significant difference was observed on PSD 42. Data are shown as means ± SEM. *$P < 0.05$. **Dashed lines** represented baseline VCAM-MPIO binding in naive animals.

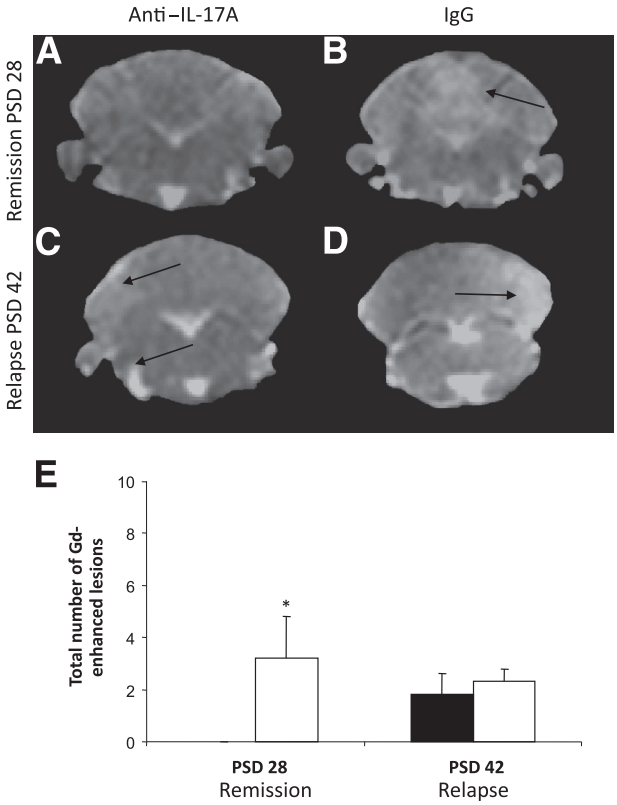

Figure 7 Quantitative analysis of VCAM-MPIO binding and Gd-DTPA enhancement. **A**—**D:** Gd-DTPA—enhancing T1-weighed images from the cerebellum of anti—IL-17A— or IgG-treated animals on PSDs 28 (**A** and **B**) and 42 (**C** and **D**). **E:** The number of Gd-DTPA—enhancing lesions (indicating BBB breakdown) in each treatment group. An increase in the number of hyperintensities was found in IgG-treated mice (white bars) compared with anti—IL-17A—treated animals (black bars) on PSD 28, but the mean number of total Gd-DTPA—enhancing lesions per animal was not different on PSD 42. Data are shown as means ± SEM. $*P < 0.05$. **Arrows** indicate Gd-DTPA-enhancing lesions.

as with VCAM-MPIO, no significant difference could be detected on PSD 42 despite the improvement in clinical signs (Figure 7). In addition, it is of note that although many lesions are visible in anti—IL-17A—treated mice using VCAM-MPIO imaging, these are undetectable using Gd-DTPA, suggesting that the former is a more sensitive modality for identifying neuropathologic features in CR-EAE.

mRNA Expression of IL-17 in the CNS Is Highest in Acute Disease Compared with Subsequent Phases

To assess the levels of IL-17A production in the CNS, 1-mm slices through the cerebellum and brain from EAE and CFA animals were collected on PSDs 10, 14, 17, 28, and 38 during the course of disease and were analyzed using quantitative RT-PCR. The expression of mRNA for IL-17A was significantly higher during the acute phase of EAE on PSD 14 compared with all other time points and with CFA controls. Thus, despite the clinically apparent therapeutic effects of anti—IL-17A, CNS mRNA expression of the cytokine returned to baseline levels by PSD 17 (Figure 8).

Discussion

This study aimed to investigate the effects of prophylactic and treatment regimens of anti—IL-17A therapy on ABH mice with CR-EAE using the conventional clinical EAE score, new behavioral tests, and neuroradiologic outcome measures. Overall, in the prophylactic and treatment regimens, anti—IL-17A therapy was shown to ameliorate clinical signs in CR-EAE ABH mice. The therapeutic efficacy observed with the prophylactic dosing regimen was particularly significant, preventing the development of acute disease and subsequent relapse and improving clinical and behavioral outcomes. However, in a more clinically relevant treatment paradigm in which anti—IL-17A was given at peak disease, the treatment ameliorated the clinical signs in the relapse phase, but the underlying radiologic findings were unaffected. Although anti—IL-17A has shown promise in early clinical trials, it will be important to discover whether it, like so many other therapies for MS, affects disease progression in the longer term.

The Importance of Enhancing the Relevance of Animal Disease Models

Developing animal models with sufficient etiologic and phenotypic relevance to their human disease counterparts raises numerous challenges. MS is an imperfectly understood demyelinating and neurodegenerative condition that affects individuals over many years, often multiple decades, causing idiosyncratic impairments of sensory, motor, autonomic, and neurocognitive functions, which may be primarily progressive or relapsing-remitting and secondarily progressive in nature. The heterogenous features of the condition, in clinical terms and pathologically, as demonstrated by inconsistent MRI morphologic changes[26] and histopathologic variation,[27,28] pose particular problems in terms of generating a truly representative animal model.

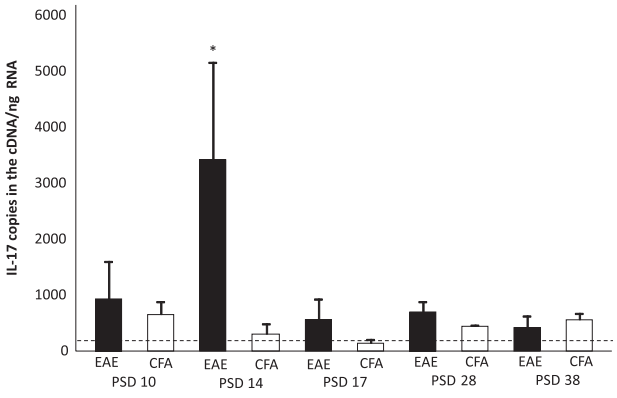

Figure 8 mRNA expression of IL-17A in the CNS was higher acutely than chronically. Real-time quantitative PCR ($n = 6$) on PSDs 10, 14, 17, and 28 revealed significantly elevated mRNA expression of IL-17A on PSD 14, during acute disease, compared with CFA mice. This expression declined by PSD 17. The horizontal dotted line indicates basal IL-17A expression in naive animals. Data are shown as means ± SEM. $*P < 0.05$.

Moreover, despite the widespread acceptance of EAE as a suitable parallel condition in animals, current methods used to assess disease severity, ie, the conventional clinical scoring system, are based on gross observation, whereas the improvements most sought after by patients with MS are in fine motor control, with a subsequent reduction in functional impairment. There is little evidence in the literature analyzing the EAE disease course using motor or behavioral tests, and previous reports have been limited by the short timeframe over which animals were examined (PSDs 0 to 20)[29] or the lengthy intervals between tests.[30]

This study is, therefore, important in its use of behavioral measures of motor function throughout the disease course, which demonstrated that the decreased clinical score in anti−IL-17A−treated mice corresponded to a functional improvement in coordination and limb control and a reduction in weakness and paralysis, a more useful assessment of CR-EAE disability. In the future, such motor tests could, therefore, be used, in conjunction with imaging and histologic studies, to provide more sensitive pretrial evaluations of therapeutic interventions.

Assessment of the Clinical-Neuropathologic Association

One of the greatest challenges in the investigation into the etiologic processes behind MS and EAE has been the dissociation between the clinical presentation of the condition and the detection of pathologic changes associated with disease activity. Current clinical guidelines include MRI in the diagnostic criteria for MS, with conventional T2-weighted MRI or passive contrast (Gd-DTPA)−enhanced T1-weighted techniques used to identify two or more characteristic neurologic lesions separated in space and time.[31]

It is well-known, however, that neither of these approaches, both of which are weighted toward the later stages of pathology, such as BBB breakdown, accurately reflects disease activity, and there is often a discrepancy between conventionally detectable lesion load and clinical score. There is, therefore, a need for methods that detect earlier disease and the underlying neuroimmunopathologic processes.

In recent years, a variety of approaches to detect early pathologic changes have been developed. Gadofluorine M, a new passive contrast agent, has been reported to reveal more MS lesions.[32] Interactions of the compound with albumin and extracellular matrix proteins result in gadofluorine-labeled myelin debris, which can subsequently be phagocytosed by macrophages. This allows for visualization of lesions by passive accumulation across a compromised BBB and by the recruitment of labeled macrophages to areas of more acute pathology when the BBB is still intact.

Alternative approaches include the use of paramagnetic myeloperoxidase sensors to detect areas of inflammatory cell infiltration[33] and ultra-small superparamagnetic particles of iron oxide to detect and quantify inflammation.[34−37] Myeloperoxidase is abundantly secreted by inflammatory cells and can activate a myeloperoxidase-paramagnetic sensor containing a Gd-DTPA molecule, reported to act as a more sensitive marker of active inflammatory lesions and correlating with increased clinical severity.[38] Similarly, i.v. administered ultra-small superparamagnetic particles of iron oxide have been shown on T2*-weighted images capable of identifying early and late active inflammatory processes in MS[39] either by passively crossing a compromised BBB or after systematic phagocytosis by macrophages that are subsequently recruited into the CNS. The latter approach has previously been used to evaluate relapse and efficacy of FTY720 treatment in a CR-EAE mouse model.[40]

The novel VCAM-MPIO contrast agent used in this study facilitates visualization and, therefore, quantification of vascular endothelial VCAM-1 expression patterns,[41] allowing for the detection of spatial and temporal changes with disease progression. Induction of cell adhesion molecule expression on the luminal endothelial surface is one of the first steps in leukocyte infiltration into the CNS; thus, this technique targets an early phase in pathogenesis, which is likely to occur before significant monocyte recruitment. During remission, reduced levels of VCAM-MPIO binding were demonstrated on the cerebral vasculature of anti−IL-17A−treated mice relative to the expression seen in IgG-treated animals. Similarly, Gd-DTPA−enhancing lesions were seen in the IgG group but not at all in anti−IL-17A animals, suggesting that VCAM-MPIO may be a more sensitive marker of disease activity than Gd-DTPA.

A further advantage of the VCAM-MPIO system is the absence of any confounding effects on immune function. For example, it is likely that phagocytosis of ultra-small superparamagnetic particles of iron oxide, as a cell marker, will alter leukocyte function and that accumulation of iron in the brain is inevitable. This is not a feature of the VCAM-MPIO approach because the particles are rapidly cleared from the circulation and target site, making the technique ideal for serial imaging studies. Moreover, the limitations of other approaches, such as a long delay between agent administration and imaging, are avoided in this technique, enhancing its practicality in a clinical context.

Neuropathologic Mechanisms Underlying Different Stages of CR-EAE Disease

Despite the advantages of VCAM-MPIO imaging, Gd-DTPA−enhancing lesions and VCAM-MPIO−induced contrast remained unchanged by anti−IL-17A treatment during the relapse phase of the study. This dissociation between MRI-determined lesion load and clinical signs may suggest that the disease processes responsible for the clinical signs are distinct from those that generate the signals currently observable by MRI and may or may not be affected by anti−IL-17A treatment. In particular, lesions in EAE models reflect not only increased endothelium VCAM-1 levels but also additional inflammatory (edema and conduction block), demyelinating, and axonal injury components, which may also be spatially and

temporally distinct. However, we have shown that VCAM-MPIO binding is associated with inflammatory foci that are also associated with demyelinating and axonal injury and where binding may or may not be associated with BBB breakdown.[19] A more likely explanation for the clinicoradiologic mismatch might be that anti−IL-17A therapy is more effective at ameliorating spinal disease, which we were unable to image. MS pathology affects the whole of the neuraxis, and it is clear that the behavioral outcomes are likely to depend more on the presence of spinal disease. We previously showed that the spinal cord mounts a more florid inflammatory response after injury and may be more tractable to therapy given that the blood−spinal cord barrier may be more penetrant as a consequence of increased numbers of inflammatory lesions.[42] However, it is becoming increasingly clear that cortical pathology[43] and diffuse extralesional axonal damage in the brain[44] are likely to contribute most to long-term disability and cognitive decline. Thus, it is important for any new therapy for MS to show disease-modifying properties in the brain. Herein, anti−IL-17A did not change the radiologic outcomes, which suggests that it might not be well suited to target MS lesions in the brain.

The number of IL-17−producing cells in the CNS in the relasping stage of the disease, ie, chronic EAE, has been shown to be lower than in acute EAE, but they are still known to be present in the periphery.[9] Others have also shown that cells with a combined T_H1/T_H17 are present in very early disease.[45] Likewise, this study demonstrated that peak CNS IL-17 mRNA expression was present in the acute disease phase, reducing with disease progression, and this may account for the increasing ineffectiveness of anti−IL-17A in affecting the MRI indices of ongoing CNS inflammation.

The distribution of inflammatory cells in the systemic and CNS compartments and the relative contribution of these cells in the disease pathogenesis remain crucial but poorly understood components. It will be of interest to discover whether IL-17−positive T cells are actively excluded from the brain during the remission and relapse periods in CR-EAE, as might be suggested in this study by the lower CNS cytokine levels during these periods.

However, this reduced relapse phase expression does not diminish the potential therapeutic validity of targeting IL-17A to reduce the relapse rate. Patients with MS generally have higher circulating peripheral cytokine and chemokine levels, and this peripheral expression may contribute to the control of leukocyte recruitment to chronic central lesions.[46] Indeed, given the effects of IL-17 on the innate immune system,[47] it seems likely that the peripheral cytokine does contribute to the mobilization and migration of peripheral leukocyte populations, although the exact mechanisms still remain to be elucidated.

Conclusions

This study demonstrated the efficacy of anti−IL-17A treatment prophylactically and as a means of reducing the severity of established clinical disease in the CR-EAE mouse model of MS. Conventional scoring and behavioral outcome measures were included, with use of the latter enhancing the relevance of EAE assessment to the clinical aspirations of patients with MS.

It has also been shown that the novel molecular MRI approach identifying endovascular VCAM-1 expression used in this study has the ability to detect clinically silent disease in remission and relapse. This highlights the need for the development of further molecular imaging tools, in mice and humans, to detect the earliest immunopathologic processes.

Supplemental Data

Supplemental material for this article can be found at *http://dx.doi.org/10.1016/j.ajpath.2013.02.029*.

References

1. Hu W, Lucchinetti CF: The pathological spectrum of CNS inflammatory demyelinating diseases. Semin Immunopathol 2009, 31:439−453
2. Fransson ME, Liljenfeldt LS, Fagius J, Totterman TH, Loskog AS: The T-cell pool is anergized in patients with multiple sclerosis in remission. Immunology 2009, 126:92−101
3. Kroenke MA, Carlson TJ, Andjelkovic AV, Segal BM: IL-12- and IL-23-modulated T cells induce distinct types of EAE based on histology, CNS chemokine profile, and response to cytokine inhibition. J Exp Med 2008, 205:1535−1541
4. Becher B, Durell BG, Noelle RJ: Experimental autoimmune encephalitis and inflammation in the absence of interleukin-12. J Clin Invest 2002, 110:493−497
5. Langrish CL, Chen Y, Blumenschein WM, Mattson J, Basham B, Sedgwick JD, McClanahan T, Kastelein RA, Cua DJ: IL-23 drives a pathogenic T cell population that induces autoimmune inflammation. J Exp Med 2005, 201:233−240
6. Huber M, Heink S, Pagenstecher A, Reinhard K, Ritter J, Visekruna A, Guralnik A, Bollig N, Jeltsch K, Heinemann C, Wittmann E, Buch T, Prazeres da Costa O, Brustle A, Brenner D, Mak TW, Mittrucker HW, Tackenberg B, Kamradt T, Lohoff M: IL-17A secretion by CD8+ T cells supports Th17-mediated autoimmune encephalomyelitis. J Clin Invest 2013, 123:247−260
7. Hofstetter HH, Ibrahim SM, Koczan D, Kruse N, Weishaupt A, Toyka KV, Gold R: Therapeutic efficacy of IL-17 neutralization in murine experimental autoimmune encephalomyelitis. Cell Immunol 2005, 237:123−130
8. Park H, Li Z, Yang XO, Chang SH, Nurieva R, Wang YH, Wang Y, Hood L, Zhu Z, Tian Q, Dong C: A distinct lineage of CD4 T cells regulates tissue inflammation by producing interleukin 17. Nat Immunol 2005, 6:1133−1141
9. Chen Y, Langrish CL, McKenzie B, Joyce-Shaikh B, Stumhofer JS, McClanahan T, Blumenschein W, Churakovsa T, Low J, Presta L, Hunter CA, Kastelein RA, Cua DJ: Anti-IL-23 therapy inhibits multiple inflammatory pathways and ameliorates autoimmune encephalomyelitis. J Clin Invest 2006, 116:1317−1326
10. Cua DJ, Sherlock J, Chen Y, Murphy CA, Joyce B, Seymour B, Lucian L, To W, Kwan S, Churakova T, Zurawski S, Wiekowski M, Lira SA, Gorman D, Kastelein RA, Sedgwick JD: Interleukin-23 rather than interleukin-12 is the critical cytokine for autoimmune inflammation of the brain. Nature 2003, 421:744−748
11. Yang Y, Weiner J, Liu Y, Smith AJ, Huss DJ, Winger R, Peng H, Cravens PD, Racke MK, Lovett-Racke AE: T-bet is essential for encephalitogenicity of both Th1 and Th17 cells. J Exp Med 2009, 206: 1549−1564

12. Haak S, Croxford AL, Kreymborg K, Heppner FL, Pouly S, Becher B, Waisman A: IL-17A and IL-17F do not contribute vitally to autoimmune neuro-inflammation in mice. J Clin Invest 2009, 119:61−69
13. Kroenke MA, Segal BM: Th17 and Th1 responses directed against the immunizing epitope, as opposed to secondary epitopes, dominate the autoimmune repertoire during relapses of experimental autoimmune encephalomyelitis. J Neurosci Res 2007, 85:1685−1693
14. Mangalam A, Luckey D, Basal E, Jackson M, Smart M, Rodriguez M, David C: HLA-DQ8 (DQB1*0302)-restricted Th17 cells exacerbate experimental autoimmune encephalomyelitis in HLA-DR3-transgenic mice. J Immunol 2009, 182:5131−5139
15. Luger D, Silver PB, Tang J, Cua D, Chen Z, Iwakura Y, Bowman EP, Sgambellone NM, Chan CC, Caspi RR: Either a Th17 or a Th1 effector response can drive autoimmunity: conditions of disease induction affect dominant effector category. J Exp Med 2008, 205:799−810
16. Kebir H, Kreymborg K, Ifergan I, Dodelet-Devillers A, Cayrol R, Bernard M, Giuliani F, Arbour N, Becher B, Prat A: Human TH17 lymphocytes promote blood-brain barrier disruption and central nervous system inflammation. Nat Med 2007, 13:1173−1175
17. Yan Y, Ding X, Li K, Ciric B, Wu S, Xu H, Gran B, Rostami A, Zhang GX: CNS-specific therapy for ongoing EAE by silencing IL-17 pathway in astrocytes. Mol Ther 2012, 20:1338−1348
18. McAteer MA, Sibson NR, von zur Muhlen C, Schneider JE, Lowe AS, Warrick N, Channon KM, Anthony DC, Choudhury RP: In vivo magnetic resonance imaging of acute brain inflammation using microparticles of iron oxide. Nat Med 2007, 13:1253−1258
19. Serres S, Mardiguian S, Campbell SJ, McAteer MA, Akhtar A, Krapitchev A, Choudhury RP, Anthony DC, Sibson NR: VCAM-1-targeted magnetic resonance imaging reveals subclinical disease in a mouse model of multiple sclerosis. FASEB J 2011, 25:4415−4422
20. Newman TA, Woolley ST, Hughes PM, Sibson NR, Anthony DC, Perry VH: T-cell- and macrophage-mediated axon damage in the absence of a CNS-specific immune response: involvement of metalloproteinases. Brain 2001, 124:2203−2214
21. Guenther K, Deacon RM, Perry VH, Rawlins JN: Early behavioural changes in scrapie-affected mice and the influence of dapsone. Eur J Neurosci 2001, 14:401−409
22. Jiang Y, Deacon R, Anthony D, Campbell S: Inhibition of peripheral TNF can block the malaise associated with CNS inflammatory diseases. Neurobiol Dis 2008, 32:125−132
23. Giacomini PS, Levesque IR, Ribeiro L, Narayanan S, Francis SJ, Pike GB, Arnold DL: Measuring demyelination and remyelination in acute multiple sclerosis lesion voxels. Arch Neurol 2009, 66: 375−381
24. Campbell SJ, Hughes PM, Iredale JP, Wilcockson DC, Waters S, Docagne F, Perry VH, Anthony DC: CINC-1 is identified as an acute-phase protein induced by focal brain injury causing leukocyte mobilization and liver injury. FASEB J 2003, 17:1168−1170
25. Campbell SJ, Perry VH, Pitossi FJ, Butchart AG, Chertoff M, Waters S, Dempster R, Anthony DC: Central nervous system injury triggers hepatic CC and CXC chemokine expression that is associated with leukocyte mobilization and recruitment to both the central nervous system and the liver. Am J Pathol 2005, 166:1487−1497
26. McFarland HF: The multiple-sclerosis lesion. Ann Neurol 1995, 37: 419−421
27. Raine CS: The neuropathology of multiple sclerosis. Edited by Raine CS, McFarland HF, Tourtellotte WW. Multiple Sclerosis: Clinical and Pathogenic Basis. London, Chapman and Hall Medical, 1997, pp 151−172
28. Lucchinetti C, Bruck W, Parisi J, Scheithauer B, Rodriguez M, Lassmann H: Heterogeneity of multiple sclerosis lesions: implications for the pathogenesis of demyelination. Ann Neurol 2000, 47:707−717
29. Buddeberg BS, Kerschensteiner M, Merkler D, Stadelmann C, Schwab ME: Behavioral testing strategies in a localized animal model of multiple sclerosis. J Neuroimmunol 2004, 153:158−170
30. Jones MV, Nguyen TT, Deboy CA, Griffin JW, Whartenby KA, Kerr DA, Calabresi PA: Behavioral and pathological outcomes in MOG 35-55 experimental autoimmune encephalomyelitis. J Neuroimmunol 2008, 199:83−93
31. McDonald WI, Compston A, Edan G, Goodkin D, Hartung HP, Lublin FD, McFarland HF, Paty DW, Polman CH, Reingold SC, Sandberg-Wollheim M, Sibley W, Thompson A, van den Noort S, Weinshenker BY, Wolinsky JS: Recommended diagnostic criteria for multiple sclerosis: guidelines from the International Panel on the diagnosis of multiple sclerosis. Ann Neurol 2001, 50:121−127
32. Wessig C, Jestaedt L, Sereda MW, Bendszus M, Stoll G: Gadofluorine M-enhanced magnetic resonance nerve imaging: comparison between acute inflammatory and chronic degenerative demyelination in rats. Exp Neurol 2008, 210:137−143
33. Breckwoldt MO, Chen JW, Stangenberg L, Aikawa E, Rodriguez E, Qiu S, Moskowitz MA, Weissleder R: Tracking the inflammatory response in stroke in vivo by sensing the enzyme myeloperoxidase. Proc Natl Acad Sci U S A 2008, 105:18584−18589
34. Brochet B, Deloire MS, Touil T, Anne O, Caille JM, Dousset V, Petry KG: Early macrophage MRI of inflammatory lesions predicts lesion severity and disease development in relapsing EAE. Neuroimage 2006, 32:266−274
35. Dousset V, Brochet B, Deloire MS, Lagoarde L, Barroso B, Caille JM, Petry KG: MR imaging of relapsing multiple sclerosis patients using ultra-small-particle iron oxide and compared with gadolinium. AJNR Am J Neuroradiol 2006, 27:1000−1005
36. Floris S, Blezer EL, Schreibelt G, Dopp E, van der Pol SM, Schadee-Eestermans IL, Nicolay K, Dijkstra CD, de Vries HE: Blood-brain barrier permeability and monocyte infiltration in experimental allergic encephalomyelitis: a quantitative MRI study. Brain 2004, 127:616−627
37. Saleh A, Wiedermann D, Schroeter M, Jonkmanns C, Jander S, Hoehn M: Central nervous system inflammatory response after cerebral infarction as detected by magnetic resonance imaging. NMR Biomed 2004, 17:163−169
38. Forghani R, Wojtkiewicz GR, Zhang Y, Seeburg D, Bautz BR, Pulli B, Milewski AR, Atkinson WL, Iwamoto Y, Zhang ER, Etzrodt M, Rodriguez E, Robbins CS, Swirski FK, Weissleder R, Chen JW: Demyelinating diseases: myeloperoxidase as an imaging biomarker and therapeutic target. Radiology 2012, 263:451−460
39. Vellinga MM, Oude Engberink RD, Seewann A, Pouwels PJ, Wattjes MP, van der Pol SM, Pering C, Polman CH, de Vries HE, Geurts JJ, Barkhof F: Pluriformity of inflammation in multiple sclerosis shown by ultra-small iron oxide particle enhancement. Brain 2008, 131:800−807
40. Rausch M, Hiestand P, Foster CA, Baumann DR, Cannet C, Rudin M: Predictability of FTY720 efficacy in experimental autoimmune encephalomyelitis by in vivo macrophage tracking: clinical implications for ultrasmall superparamagnetic iron oxide-enhanced magnetic resonance imaging. J Magn Reson Imaging 2004, 20:16−24
41. van Kasteren SI, Campbell SJ, Serres S, Anthony DC, Sibson NR, Davis BG: Glyconanoparticles allow pre-symptomatic in vivo imaging of brain disease. Proc Natl Acad Sci U S A 2009, 106:18−23
42. Schnell L, Fearn S, Schwab ME, Perry VH, Anthony DC: Cytokine-induced acute inflammation in the brain and spinal cord. J Neuropathol Exp Neurol 1999 Mar, 58(3):245−254
43. Popescu BF, Lucchinetti CF: Meningeal and cortical grey matter pathology in multiple sclerosis. BMC Neurol 2012, 12:11
44. Howell OW, Rundle JL, Garg A, Komada M, Brophy PJ, Reynolds R: Activated microglia mediate axoglial disruption that contributes to axonal injury in multiple sclerosis. J Neuropathol Exp Neurol 2010, 69:1017−1033
45. Murphy AC, Lalor SJ, Lynch MA, Mills KH: Infiltration of Th1 and Th17 cells and activation of microglia in the CNS during the course of experimental autoimmune encephalomyelitis. Brain Behav Immun 2010, 24:641−651
46. Campbell SJ, Meier U, Mardiguian S, Jiang Y, Littleton ET, Bristow A, Relton J, Connor TJ, Anthony DC: Sickness behaviour is induced by a peripheral CXC-chemokine also expressed in Multiple Sclerosis and EAE. Brain Behav Immun 2010, 24:738−746
47. Iwakura Y, Ishigame H, Saijo S, Nakae S: Functional specialization of interleukin-17 family members. Immunity 2011, 34:149−162